

## Closed-form analytical model of the electron whistler and cyclotron maser instabilities in relativistic plasma with arbitrary energy anisotropy

Peter H. Yoon and Ronald C. Davidson

*Plasma Fusion Center, Massachusetts Institute of Technology, Cambridge, Massachusetts 02139*

(Received 21 August 1986)

Detailed properties of the cyclotron maser and whistler instabilities in a relativistic magnetized plasma are investigated for a particular choice of anisotropic distribution function  $F(p_{\perp}^2, p_z)$  that permits an exact analytical reduction of the dispersion relation for arbitrary energy anisotropy. The analysis assumes electromagnetic wave propagation parallel to a uniform applied magnetic field  $B_0 \hat{e}_z$ . Moreover, the particular equilibrium distribution function considered in the present analysis assumes that all electrons move on a surface with perpendicular momentum  $p_{\perp} = \hat{p}_{\perp} = \text{const}$  and are uniformly distributed in axial momentum from  $p_z = -\hat{p}_z = \text{const}$  to  $p_z = +\hat{p}_z = \text{const}$  (so-called "waterbag" distribution in  $p_z$ ). This distribution function incorporates the effects of a finite momentum spread in the parallel direction. The resulting dispersion relation is solved numerically, and detailed properties of the cyclotron maser and whistler instabilities are determined over a wide range of energy anisotropy, normalized density  $\omega_p^2/\omega_c^2$ , and electron energy.

### I. INTRODUCTION

The classical cyclotron maser<sup>1-16</sup> and electron whistler<sup>16-20</sup> instabilities in a uniform plasma are transverse electromagnetic instabilities<sup>20-22</sup> driven by an anisotropy in the average kinetic energy of the constituent electrons. These instabilities have a wide range of applicability to astrophysical and space plasmas,<sup>3-14,18</sup> to laboratory plasmas with intense rf heating,<sup>16,19</sup> and to relativistic electron beams used for microwave generation.<sup>1,2,15</sup> Since the late 1950's (see citations in Ref. 1), the cyclotron maser instability has been the subject of ongoing research. In astrophysical applications, Jupiter's decametric radio emission<sup>3,4</sup> and Earth's auroral kilometric radiation<sup>3,4</sup> have been attributed to the cyclotron maser instability. In laboratory experiments,<sup>1,2,15</sup> a very notable application is to the gyrotron device, used for coherent radiation generation. The electron whistler instability was first investigated by Sudan<sup>17</sup> in the nonrelativistic regime. Recent studies of the whistler instability by Gladd<sup>19</sup> have included relativistic effects.

For *nonrelativistic* anisotropic plasma, detailed properties of the whistler instability<sup>20</sup> are readily calculated for a wide range of distribution functions  $F(p_{\perp}^2, p_z)$ . Here, we assume electromagnetic wave propagation parallel to a uniform applied magnetic field  $B_0 \hat{e}_z$ , and the terms "perpendicular" and "parallel" refer to directions relative to  $B_0 \hat{e}_z$ . For *relativistic* anisotropic plasma, however, because of the coupling of the perpendicular and parallel particle motions through the relativistic mass factor  $\gamma = (1 + p_{\perp}^2/m^2c^2 + p_z^2/m^2c^2)^{1/2}$ , properties of the cyclotron maser and whistler instabilities are usually calculated in limiting regimes which allow approximate analytical solutions or substantial simplification of the electromagnetic dispersion relation. These limiting regimes range from weak energy anisotropy, to very strong energy anisotropy, to long perturbation wavelengths, to short perturbation wavelengths. Moreover, the distribution functions used in the analyses of these instabilities range typically from a weakly relativistic loss-cone (Dory-Guest-Harris) distribution,<sup>3-14</sup> to monoenergetic equilibria<sup>1,2,15</sup> in which the influence of a spread in parallel or perpendicular momentum is neglected. While the DGH distribution may represent a realistic model for the particular applications considered in Refs. 3-14, these analyses<sup>3-14</sup> are restricted to mildly relativistic electrons.

The purpose of this paper is to investigate detailed properties of the cyclotron maser and whistler instabilities in relativistic magnetized plasma for a particular choice of anisotropic distribution function that permits an *exact* analytical reduction of the dispersion relation for arbitrary energy and arbitrary energy anisotropy. This calculation is intended to provide qualitative insights regarding stability behavior for more general choices of equilibrium distribution function. The particular distribution function<sup>22</sup> [Eq. (7)] considered in the present analysis assumes that all electrons move on a surface with perpendicular momentum  $p_{\perp} = \hat{p}_{\perp} = \text{const}$ , and are uniformly distributed in parallel momentum between  $p_z = -\hat{p}_z = \text{const}$  and  $p_z = +\hat{p}_z = \text{const}$ . (so-called "waterbag" distribution in  $p_z$ ). This distribution function incorporates the effects of a finite momentum spread in the parallel direction. For this choice of  $F(p_{\perp}^2, p_z)$ , the integrations over  $p_{\perp}$  and  $p_z$  in the dispersion relation [Eq. (2)] can be carried out in closed form. The resulting dispersion relation [Eq. (19)] is valid for arbitrary energy anisotropy  $\hat{\beta}_{\perp}^2/2\hat{\beta}_z^2$  and can be used to investigate detailed stability properties over a wide range of system parameters. Here,  $\hat{\beta}_{\perp}$  and  $\hat{\beta}_z$  are defined by  $\hat{\beta}_{\perp} = \hat{p}_{\perp}/\hat{\gamma}mc$  and  $\hat{\beta}_z = \hat{p}_z/\hat{\gamma}mc$ , where  $\hat{\gamma} = (1 + \hat{p}_{\perp}^2/m^2c^2 + \hat{p}_z^2/m^2c^2)^{1/2}$ . Although the present stability analysis is restricted to parallel propagation (i.e.,  $k_{\perp} = 0$  is assumed), the calculation does allow for arbitrary electron

energy and is not restricted to weakly relativistic electrons.<sup>3-14</sup>

The organization of this paper is the following. In Sec. II we outline the theoretical model (Sec. IIA), derive the electromagnetic dispersion relation (19) for the choice of equilibrium distribution function in Eq. (7) (Sec. IIB), and (for completeness), show that Eq. (19) reduces to familiar results in the two limiting cases  $\hat{\beta}_z=0$  and  $B_0=0$  (Sec. IIC). In Sec. III the dispersion relation (19) is solved numerically, and detailed stability properties are investigated for both the cyclotron maser and whistler instabilities over a wide range of system parameters  $\hat{\beta}_1^2/2\hat{\beta}_z^2$ ,  $\omega_p^2/\omega_c^2$ ,  $\hat{\gamma}$ , and  $ck_z/\omega_p$ . Here,  $\omega_c=eB_0/mc$  and  $\omega_p=(4\pi\hat{n}e^2/m)^{1/2}$  are the nonrelativistic electron cyclotron and plasma frequencies, respectively, and  $k_z$  is the axial wave number of the perturbation. Finally, in Sec. IV we obtain the electromagnetic dispersion relation [Eq. (35)] for the case where the distribution in parallel momentum  $p_z$  corresponds to thermal equilibrium [Eq. (29)].

$$0=D_T^\pm(\omega, k_z)=1-\frac{c^2k_z^2}{\omega^2}+\frac{\omega_p^2}{\omega^2}\int\frac{d^3p}{\gamma}\frac{(p_\perp/2)}{\gamma\omega-k_zp_z/m\pm\omega_c}\left[\left(\gamma\omega-\frac{k_zp_z}{m}\right)\frac{\partial}{\partial p_\perp}+\frac{k_zp_\perp}{m}\frac{\partial}{\partial p_z}\right]F(p_\perp^2, p_z), \quad (2)$$

where  $k_z$  is the axial wave number and  $\omega$  is the complex oscillation frequency with  $\text{Im}\omega>0$ , which corresponds to instability (temporal growth). In Eq. (2)  $\omega_p^2=4\pi\hat{n}e^2/m$  is the nonrelativistic plasma frequency squared;  $\omega_c=eB_0/mc$  is the nonrelativistic cyclotron frequency;  $-e$  and  $m$  are the electron charge and rest mass, respectively;  $c$  is the speed of light in *vacuo*;  $\gamma=(1+p_\perp^2/m^2c^2+p_z^2/m^2c^2)^{1/2}$  is the relativistic mass factor; the range of integration is  $\int d^3p\cdots=2\pi\int_0^\infty dp_\perp p_\perp\int_{-\infty}^\infty dp_z\cdots$ ; and the normalization of  $F$  is  $\int d^3p F(p_\perp^2, p_z)=1$ . Moreover, the two signs in Eq. (2) refer to electromagnetic waves with right-circular polarization ( $-$  sign) and left-circular polarization ( $+$  sign), respectively. The dispersion relation (2) is readily extended to the case of a multicomponent plasma by making the replacements  $\omega_p^2\cdots\rightarrow\sum_j\omega_{pj}^2\cdots$ ,  $F(p_\perp^2, p_z)\rightarrow F_j(p_\perp^2, p_z)$ ,  $\omega_c\rightarrow\omega_{cj}$ , etc., where  $j$  labels the plasma species.

The dispersion relation (2) can be used to investigate detailed electromagnetic stability properties for a wide range of anisotropic distribution functions  $F(p_\perp^2, p_z)$ . For *rela-*

## II. THEORETICAL MODEL AND DISPERSION RELATION

### A. Electromagnetic dispersion relation

In the present analysis we specialize to the case of stationary ions ( $m_i\rightarrow\infty$ ) and consider a single active component of relativistic anisotropic electrons. Electromagnetic stability properties are investigated for perturbations propagating in the  $z$  direction parallel to a uniform applied magnetic field  $B_0\hat{e}_z$ . Perturbations are about the class of spatially uniform equilibria with distribution function

$$f^0(\mathbf{p})=\hat{n}F(p_\perp^2, p_z), \quad (1)$$

where  $\hat{n}=\text{const}$  is the ambient electron density,  $p_\perp=(p_x^2+p_y^2)^{1/2}$  is the particle momentum perpendicular to the magnetic field  $B_0\hat{e}_z$ , and  $p_z$  is the parallel momentum. The linear dispersion relation for circularly polarized electromagnetic wave perturbations propagating in the  $z$  direction is given by

*tivistic* anisotropic plasma, we note that the perpendicular and parallel particle motions in Eq. (2) are inexorably coupled through the relativistic mass factor  $\gamma=(1+p_\perp^2/m^2c^2+p_z^2/m^2c^2)^{1/2}$ . For present purposes, we assume that the electrons move on a surface with constant perpendicular momentum  $p_\perp=\hat{p}_1=\text{const}$ . That is,  $F(p_\perp^2, p_z)$  is assumed to have the form

$$F(p_\perp^2, p_z)=\frac{1}{2\pi p_\perp}\delta(p_\perp-\hat{p}_1)F_1(p_z), \quad (3)$$

where  $F_1(p_z)$  is the parallel momentum distribution (yet unspecified) with normalization  $\int_{-\infty}^\infty dp_z F_1(p_z)=1$ . The strongly peaked distribution in  $p_\perp$  in Eq. (3) can occur in laboratory plasmas when there is intense microwave heating (e.g., electron cyclotron resonance heating) of the electrons perpendicular to  $B_0\hat{e}_z$ .

The integration over  $p_\perp$  in Eq. (2) can be carried out in closed analytical form for the choice of distribution function in Eq. (3). Making use of  $\partial\gamma/\partial p_z=p_z/\gamma m^2c^2$  and  $\partial\gamma/\partial p_\perp=p_\perp/\gamma m^2c^2$ , some straightforward algebra shows that Eq. (2) can be expressed as

$$0=D_T^\pm(\omega, k_z)=1-\frac{c^2k_z^2}{\omega^2}-\frac{\omega_p^2}{\omega^2}\int_{-\infty}^\infty\frac{dp_z}{\gamma}F_1(p_z)\left[\frac{\gamma-k_zp_z/m\omega}{\gamma-k_zp_z/m\omega\pm\omega_c/\omega}-\frac{\hat{p}_1^2}{2m^2c^2}\frac{(1-c^2k_z^2/\omega^2)}{(\gamma-k_zp_z/m\omega\pm\omega_c/\omega)^2}\right]. \quad (4)$$

In Eq. (4)  $\gamma$  is defined by

$$\gamma=\left[1+\frac{\hat{p}_1^2}{m^2c^2}+\frac{p_z^2}{m^2c^2}\right]^{1/2}, \quad (5)$$

where  $p_\perp$  has been replaced by  $\hat{p}_1=\text{const}$ .

### B. Waterbag distribution in parallel momentum

The dispersion relation (4) can be used to investigate detailed electromagnetic stability properties for a wide range of distribution functions  $F_1(p_z)$ . For purposes of elucidating the essential features of the instability in relativistic anisotropic plasma, we make a particular choice of

$F_1(p_z)$  for which the integrations over  $p_z$  in Eq. (4) can be carried out in closed analytical form. In particular, it is assumed that the electrons are uniformly distributed in parallel momentum between  $p_z = -\hat{p}_z = \text{const}$  and  $p_z = +\hat{p}_z = \text{const}$ . That is,  $F_1(p_z)$  is specified by<sup>22</sup>

$$F_1(p_z) = \frac{1}{2\hat{p}_z} H(\hat{p}_z^2 - p_z^2), \quad (6)$$

where  $H(x)$  is the Heaviside step function defined by  $H(x) = +1$  for  $x > 0$ , and  $H(x) = 0$  for  $x < 0$ . Note from Eq. (6) that  $\int_{-\infty}^{\infty} dp_z F_1(p_z) = 1$ . Because the electrons are uniformly distributed in parallel momentum for  $|p_z| < \hat{p}_z$ , we refer to the  $p_z$  dependence of the distribution function in Eq. (6) as a waterbag distribution in  $p_z$ . Combining Eqs. (3) and (6), the total distribution function  $F(p_\perp^2, p_z)$  can be expressed as

$$F(p_\perp^2, p_z) = \frac{1}{2\pi p_\perp} \delta(p_\perp - \hat{p}_\perp) \frac{1}{2\hat{p}_z} H(\hat{p}_z^2 - p_z^2). \quad (7)$$

For future reference, we first calculate the energy anisotropy associated with the distribution function in Eq. (7).

*Equilibrium properties:* For the choice of distribution function in Eq. (7), it is useful to introduce the maximum energy  $\hat{\gamma}mc^2$ , parallel speed  $c\hat{\beta}_z$ , and perpendicular speed  $c\hat{\beta}_\perp$  defined by

$$\begin{aligned} \hat{\beta}_z &= \frac{\hat{p}_z}{\hat{\gamma}mc}, \quad \hat{\beta}_\perp = \frac{\hat{p}_\perp}{\hat{\gamma}mc}, \\ \hat{\gamma} &= \left[ 1 + \frac{\hat{p}_\perp^2}{m^2c^2} + \frac{\hat{p}_z^2}{m^2c^2} \right]^{1/2} \\ &= (1 - \hat{\beta}_\perp^2 - \hat{\beta}_z^2)^{-1/2}. \end{aligned} \quad (8)$$

We further introduce the effective "temperatures" (average momentum fluxes) in the perpendicular and parallel directions defined by

$$\begin{aligned} T_\perp &= \int d^3p \frac{p_\perp^2}{2\gamma m} F(p_\perp^2, p_z), \\ \frac{1}{2} T_z &= \int d^3p \frac{p_z^2}{2\gamma m} F(p_\perp^2, p_z). \end{aligned} \quad (9)$$

Substituting Eq. (7) into Eq. (9) and carrying out the required integrations over  $p_\perp$  and  $p_z$  give

$$\begin{aligned} T_\perp &= \frac{1}{2} \hat{\gamma} mc^2 \hat{\beta}_\perp^2 G(\hat{\beta}_z), \\ T_z &= \frac{1}{2} \hat{\gamma} mc^2 [1 - G(\hat{\beta}_z) + \hat{\beta}_z^2 G(\hat{\beta}_z)], \end{aligned} \quad (10)$$

where  $G(\hat{\beta}_z)$  is defined by

$$G(\hat{\beta}_z) = \frac{1}{2\hat{\beta}_z} \ln \left[ \frac{1 + \hat{\beta}_z}{1 - \hat{\beta}_z} \right]. \quad (11)$$

From Eq. (11) and Fig. 1 we note that  $G(\hat{\beta}_z)$  is a slowly increasing function of  $\hat{\beta}_z$  with  $G(\hat{\beta}_z) = 1 + \hat{\beta}_z^2/3 + \dots$  for  $\hat{\beta}_z \ll 1$ . Moreover, in the limit of a nonrelativistic plasma with  $\hat{\beta}_z^2 \ll 1$  and  $\hat{\beta}_\perp^2 \ll 1$ , Eq. (10) reduces to the expected results,  $T_\perp \rightarrow \frac{1}{2} mc^2 \hat{\beta}_\perp^2$  and  $T_z \rightarrow \frac{1}{3} mc^2 \hat{\beta}_z^2$ . Depending on the relative values of  $\hat{\beta}_\perp$  and  $\hat{\beta}_z$ , it is clear that the choice of distribution function in Eq. (7) can cover a wide range of energy anisotropy.

*Dispersion relation:* We now simplify the dispersion relation (4) for the choice of waterbag distribution  $F_1(p_z)$  in Eq. (6). In this regard, it is convenient to define

$$\hat{\gamma}_\perp = \left[ 1 + \frac{\hat{p}_\perp^2}{m^2c^2} \right]^{1/2} \quad (12)$$

and rewrite the expression for  $\gamma = (1 + \hat{p}_\perp^2/m^2c^2 + p_z^2/m^2c^2)^{1/2}$  in Eq. (5) as

$$\gamma = \hat{\gamma}_\perp \left[ 1 + \frac{p_z^2}{\hat{\gamma}_\perp^2 m^2 c^2} \right]^{1/2}. \quad (13)$$

In the dispersion relation (4) we change variables from  $p_z$  to  $\alpha$  where

$$p_z = (\hat{\gamma}_\perp mc) \sinh \alpha. \quad (14)$$

From Eqs. (13) and (14) it follows that

$$\begin{aligned} \gamma &= \hat{\gamma}_\perp \cosh \alpha, \\ \frac{dp_z}{\gamma} &= mc d\alpha. \end{aligned} \quad (15)$$

Substituting Eqs. (6), (14), and (15) into the dispersion relation (4) then gives

$$\begin{aligned} 0 = D_T^\pm(\omega, k_z) &= 1 - \frac{c^2 k_z^2}{\omega^2} - \frac{\omega_p^2}{\omega^2} \frac{mc}{2\hat{\beta}_z} \int_{-\hat{\alpha}}^{\hat{\alpha}} d\alpha \left[ \frac{[\cosh \alpha - (k_z c / \omega) \sinh \alpha]}{[\cosh \alpha - (k_z c / \omega) \sinh \alpha \pm \omega_c / \hat{\gamma}_\perp \omega]} \right. \\ &\quad \left. - \frac{\hat{p}_\perp^2}{2\hat{\gamma}_\perp^2 m^2 c^2} \frac{(1 - c^2 k_z^2 / \omega^2)}{[\cosh \alpha - (k_z c / \omega) \sinh \alpha \pm \omega_c / \hat{\gamma}_\perp \omega]^2} \right], \end{aligned} \quad (16)$$

where  $\hat{\gamma}_\perp = (1 + \hat{p}_\perp^2/m^2c^2)^{1/2}$  is defined in Eq. (12). The limits of integration ( $\pm \hat{\alpha}$ ) in Eq. (16) are determined from  $\hat{p}_z = (\hat{\gamma}_\perp mc) \sinh \hat{\alpha}$ . Because  $\hat{\gamma} = \hat{\gamma}_\perp \cosh \hat{\alpha}$ , where  $\hat{\gamma}$  is defined in Eq. (8), the equation determining  $\hat{\alpha}$  can also be expressed as

$$\hat{\beta}_z = \frac{\hat{p}_z}{\hat{\gamma} mc} = \tanh \hat{\alpha}. \quad (17)$$

Solving Eq. (17) for  $\hat{\alpha}$  in terms of  $\hat{\beta}_z$  gives

$$\hat{\alpha} = \frac{1}{2} \ln \left[ \frac{1 + \hat{\beta}_z}{1 - \hat{\beta}_z} \right]. \quad (18)$$

The integration over  $\alpha$  in Eq. (16) can be carried out in closed analytical form (see the Appendix). Substituting Eqs. (A4), (A6), and (A7) into Eq. (16) gives the desired dispersion relation

$$0 = D_T^\pm(\omega, k_z) = 1 - \frac{c^2 k_z^2}{\omega^2} - \frac{\omega_p^2 / \hat{\gamma}}{\omega^2} \left[ G(\hat{\beta}_z) \mp \frac{\omega_c / \hat{\gamma}}{\omega(1 - \hat{\beta}_z^2) \pm \omega_c / \hat{\gamma}} G(\xi^\pm) \right. \\ \left. - \frac{\hat{\beta}_1^2}{2} \frac{(c^2 k_z^2 - \omega^2)}{(\omega_c / \hat{\gamma})^2 + (1 - \hat{\beta}_z^2)(c^2 k_z^2 - \omega^2)} \left[ \frac{\omega(\omega \pm \omega_c / \hat{\gamma}) - c^2 k_z^2}{(\omega \pm \omega_c / \hat{\gamma})^2 - c^2 k_z^2 \hat{\beta}_z^2} \right. \right. \\ \left. \left. \mp \frac{\omega_c / \hat{\gamma}}{\omega(1 - \hat{\beta}_z^2) \pm \omega_c / \hat{\gamma}} G(\xi^\pm) \right] \right], \quad (19)$$

where  $\xi^\pm$  is defined by

$$\xi^\pm = \frac{\hat{\beta}_z [(\omega_c / \hat{\gamma})^2 + (1 - \hat{\beta}_z^2)(c^2 k_z^2 - \omega^2)]^{1/2}}{\omega(1 - \hat{\beta}_z^2) \pm \omega_c / \hat{\gamma}}, \quad (20)$$

and  $G(\xi)$  is defined by

$$G(\xi) = \frac{1}{2\xi} \ln \left[ \frac{1 + \xi}{1 - \xi} \right]. \quad (21)$$

In Eq. (19) the various quantities are defined by  $\hat{\beta}_1 = \hat{p}_1 / \hat{\gamma} mc$  [Eq. (8)],  $\hat{\beta}_z = \hat{p}_z / \hat{\gamma} mc$  [Eq. (8)],  $\hat{\gamma} = (1 + \hat{p}_1^2 / m^2 c^2 + \hat{p}_z^2 / m^2 c^2)^{1/2}$  [Eq. (8)], and  $G(\hat{\beta}_z)$  is defined in Eq. (11). The fully relativistic dispersion relation (19) can be used to investigate detailed properties of the electron whistler and cyclotron maser instabilities for a wide range of effective energy anisotropy  $\hat{\beta}_1^2 / 2\hat{\beta}_z^2$ , normalized density  $\omega_p^2 / \omega_c^2$ , electron energy  $\hat{\gamma} mc^2$ , etc.

Because  $F_1(p_z)$  is an even function of  $p_z$  in Eqs. (6) and (7), it follows that the average flow velocity in the  $z$  direction is  $V_d \equiv \int d^3 p (p_z / \gamma m) F(p_1^2, p_z) = 0$ . For electrons

with average axial velocity  $V_d \equiv \text{const} \neq 0$ , the corresponding dispersion relation for a displaced waterbag distribution is readily derived from Eq. (19) by making the appropriate Lorentz transformation of  $\omega$  and  $k_z$ . In particular, we view Eq. (19) as the dispersion equation relating  $\omega$  and  $k_z$  in a frame of reference moving with axial velocity  $V_d$  relative to the laboratory. Then the corresponding dispersion equation relating  $\omega'$  and  $k_z'$  in the *laboratory frame* is obtained by making the transformation

$$\omega = \gamma_d (\omega' - k_z' V_d), \quad (22)$$

$$k_z = \gamma_d (k_z' - \omega' V_d / c^2),$$

in Eqs. (19) and (20). Here,  $\gamma_d$  is defined by  $\gamma_d = (1 - V_d^2 / c^2)^{-1/2}$ , and  $\omega^2 - c^2 k_z^2 \rightarrow (\omega')^2 - c^2 (k_z')^2$ ;  $\omega \mp \omega_c / \hat{\gamma} \rightarrow \gamma_d (\omega' - k_z' V_d \mp \omega_c / \hat{\gamma} \gamma_d)$ ; etc.

For completeness, it is useful to simplify Eq. (19) in various limiting regimes.

### C. Limiting forms of dispersion relation

We consider the full dispersion relation (19) in two limiting cases: (a) zero parallel temperature ( $\hat{\beta}_z = 0$ ), and (b) zero magnetic field ( $B_0 = 0$ ).

*Zero parallel temperature:* For  $\hat{\beta}_z = 0$ , the case of maximum energy anisotropy, we obtain  $G(\hat{\beta}_z) \rightarrow 1$  [Eq. (11)],  $\hat{\gamma} \rightarrow \hat{\gamma}_1$  [Eq. (8)], and  $G(\xi^\pm) \rightarrow 1$  [Eq. (21)]. For  $\hat{\beta}_z \rightarrow 0$ , the dispersion relation (19) reduces to<sup>1</sup>

$$0 = D_T^\pm(\omega, k_z) \\ = 1 - \frac{c^2 k_z^2}{\omega^2} \\ - \frac{\omega_p^2 / \hat{\gamma}_1}{\omega(\omega \pm \omega_c / \hat{\gamma}_1)} \left[ 1 + \frac{\hat{\beta}_1^2}{2} \frac{(c^2 k_z^2 - \omega^2)}{\omega(\omega \pm \omega_c / \hat{\gamma}_1)} \right]. \quad (23)$$

*Zero magnetic field:* In the case where  $B_0 = 0$  and the perpendicular and parallel motions are allowed to be relativistic, we set  $\omega_c = 0$  in Eq. (19), which gives the dispersion relation<sup>22</sup>

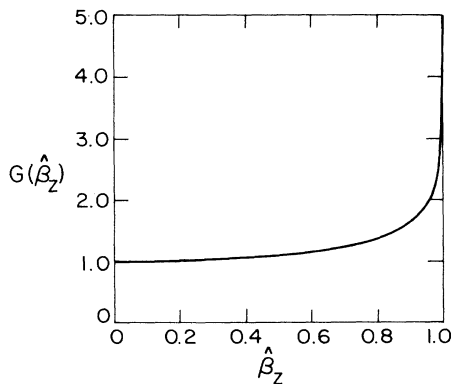


FIG. 1. Plot of  $G(\hat{\beta}_z)$  vs  $\hat{\beta}_z$  [Eq. (11)].

$$\begin{aligned}
0 &= D_{\mp}^{\pm}(\omega, k_z) \\
&= 1 - \frac{c^2 k_z^2}{\omega^2} \\
&\quad - \frac{\omega_p^2 / \hat{\gamma}}{\omega^2} \left[ G(\hat{\beta}_z) - \frac{\hat{\beta}_1^2}{2(1 - \hat{\beta}_z^2)} \left( \frac{\omega^2 - c^2 k_z^2}{\omega^2 - c^2 k_z^2 \hat{\beta}_z^2} \right) \right]. \quad (24)
\end{aligned}$$

Equation (24) gives the familiar Weibel instability<sup>21,22</sup> in the field-free case. Of course, for  $\omega_c = 0$  and  $\hat{\beta}_z = 0$ , Eqs. (23) and (24) are identical.

### III. ELECTROMAGNETIC STABILITY PROPERTIES

In this section we investigate the detailed stability properties predicted by the electromagnetic dispersion relation (19) for a wide range of effective energy anisotropy  $\hat{\beta}_1^2/2\hat{\beta}_z^2$ , normalized density  $\omega_p^2/\omega_c^2$ , and electron energy  $\hat{\gamma}mc^2$ . As a reference case, we first consider the case of extreme energy anisotropy where  $\hat{\beta}_z = 0$ . That is, the thermal speed in the  $z$  direction is effectively zero.

#### A. Extreme energy anisotropy ( $\hat{\beta}_z = 0$ )

For  $\hat{\beta}_z = 0$ , the full dispersion relation (19) reduces to Eq. (23), which can be expressed in the equivalent form<sup>1</sup>

$$(\omega^2 - c^2 k_z^2) \left[ 1 + \frac{\hat{\beta}_1^2}{2} \frac{\omega_p^2 / \hat{\gamma}_1}{(\omega - \omega_c / \hat{\gamma}_1)^2} \right] = \frac{\omega}{\omega - \omega_c / \hat{\gamma}_1} \frac{\omega_p^2}{\hat{\gamma}_1}. \quad (25)$$

In Eq. (25), without loss of generality, we have restricted attention to the branch with right-circular polarization [lower sign in Eq. (23)].

For  $\hat{\beta}_1^2 = 0$  (cold-plasma limit) Eq. (25) supports only stable oscillations ( $\text{Im}\omega = 0$ ) corresponding to a fast-wave branch, and a slow-wave branch which we refer to as the "whistler" mode or the "cyclotron" mode in the present analysis.<sup>20</sup>

For  $\hat{\beta}_1^2 \neq 0$ , however, and moderate electron density,

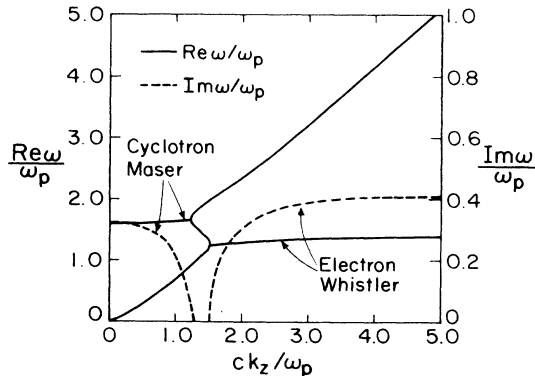


FIG. 2. Plots vs  $ck_z/\omega_p$  of  $\text{Re}\omega/\omega_p$  and  $\text{Im}\omega/\omega_p$  for the cyclotron maser and whistler instabilities obtained from Eq. (25) for  $\hat{\beta}_z = 0$ ,  $\omega_p^2/\omega_c^2 = 0.25$ , and  $\hat{\beta}_1^2 = 0.5$ .

both the fast-wave branch and the whistler mode exhibit instability in Eq. (25). In particular, it is found (Fig. 2) that the fast-wave branch becomes unstable at long axial wavelengths (sufficiently small values of  $c^2 k_z^2/\omega_p^2$ ), whereas the whistler mode becomes unstable at short axial wavelengths (sufficiently large values of  $c^2 k_z^2/\omega_p^2$ ). The unstable fast-wave mode is referred to as the *cyclotron maser instability*, whereas the unstable whistler mode is referred to as the *whistler instability*. Typical numerical results obtained from Eq. (25) are illustrated in Fig. 2 where  $\text{Re}\omega/\omega_p$  and  $\text{Im}\omega/\omega_p$  are plotted versus  $ck_z/\omega_p$  for  $\omega_p^2/\omega_c^2 = 0.25$  and  $\hat{\beta}_1^2 = 0.5$ . For specified values of  $\omega_p^2/\omega_c^2$  and  $\hat{\beta}_1^2$ , a striking feature of Fig. 2 is that the real frequency  $\text{Re}\omega$  remains approximately constant over the range of unstable wave numbers ( $k_z$ ) for both the whistler and cyclotron maser instabilities. Moreover, for  $\hat{\beta}_z = 0$ , it is evident from Fig. 2 that maximum growth rate of the whistler instability occurs for  $c^2 k_z^2/\omega_p^2 \gg 1$ . Taking  $c^2 k_z^2 \rightarrow \infty$  in the dispersion relation readily gives

$$\begin{aligned}
(\text{Im}\omega)_{\text{max}} &= \left[ \frac{\hat{\beta}_1^2}{2\hat{\gamma}_1} \right]^{1/2} \omega_p, \\
(\text{Re}\omega)_{\text{max}} &= \omega_c / \hat{\gamma}_1, \quad (26)
\end{aligned}$$

for the whistler instability at maximum growth. In units of  $\omega_p$ , it follows from Eq. (26) and  $\hat{\gamma}_1 = (1 - \hat{\beta}_1^2)^{-1/2}$  that the maximum whistler growth rate assumes its absolute maximum value of  $0.439\omega_p$  for  $\hat{\beta}_1^2 = \frac{2}{3}$  (Fig. 3). In contrast, for  $\hat{\beta}_z = 0$  and  $k_1 = 0$ , maximum growth of the cyclotron maser instability occurs for  $k_z = 0$  (Fig. 2). Moreover, the bandwidth of the cyclotron maser instability is restricted to the wave-number range  $c^2 k_z^2/\omega_p^2 \lesssim O(1)$  for the choice of parameters in Fig. 2.

For  $\hat{\beta}_1^2 \neq 0$ , and sufficiently large values of  $\omega_p^2/\omega_c^2$ , it is found from Eq. (25) that the cyclotron maser instability is completely stabilized, whereas the whistler mode remains unstable. The density threshold for stabilization of the cyclotron maser instability can be calculated exactly in terms of  $\hat{\beta}_1^2$  from Eq. (25). We take  $k_z = 0$  in Eq. (25),

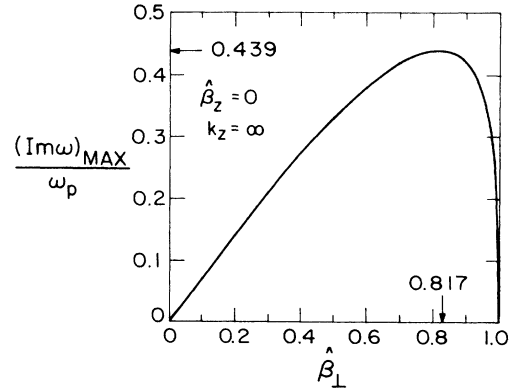


FIG. 3. Plot of normalized maximum growth rate  $(\text{Im}\omega)_{\text{max}}/\omega_p$  vs  $\hat{\beta}_1^2$  for the electron whistler branch obtained from Eq. (26) for  $\hat{\beta}_z = 0$  and  $k_z = \infty$ . The absolute maximum growth rate is  $0.439\omega_p$ , which occurs for  $\hat{\beta}_1^2 = \frac{2}{3}$ .

which corresponds to maximum growth rate of the cyclotron maser instability<sup>1</sup> when  $\hat{\beta}_z=0$  and  $k_\perp=0$ . This gives

$$0 = (\omega - \omega_c / \hat{\gamma}_\perp)^3 + \frac{\omega_c}{\hat{\gamma}_\perp} (\omega - \omega_c / \hat{\gamma}_\perp)^2 + \frac{\omega_p^2}{\hat{\gamma}_\perp} \left[ \frac{\hat{\beta}_\perp^2}{2} - 1 \right] (\omega - \omega_c / \hat{\gamma}_\perp) + \frac{\omega_c}{\hat{\gamma}_\perp} \frac{\omega_p^2}{\hat{\gamma}_\perp} \frac{\hat{\beta}_\perp^2}{2}. \quad (27)$$

Equation (27) determines the real frequency  $\text{Re}\omega$  and growth rate  $\text{Im}\omega$  of the cyclotron maser instability at maximum growth. Some straightforward algebra shows that the necessary and sufficient condition for stability ( $\text{Im}\omega=0$ ) is given by

$$\begin{aligned} \frac{\omega_p^2}{\omega_c^2} &\geq \frac{\omega_p^2}{\omega_c^2} \Big|_{\text{cr}} \\ &\equiv \frac{(1 - \hat{\beta}_\perp^2)^{1/2}}{(2 - \hat{\beta}_\perp^2)^3} [2\hat{\beta}_\perp^4 + 10\hat{\beta}_\perp^2 - 1 \\ &\quad + (64\hat{\beta}_\perp^6 + 48\hat{\beta}_\perp^4 + 12\hat{\beta}_\perp^2 + 1)^{1/2}]. \end{aligned} \quad (28)$$

That is, whenever  $\omega_p^2/\omega_c^2$  exceeds the critical value in Eq. (28), the cyclotron maser instability is completely stabilized. This is illustrated in Fig. 4, which shows the regions of  $(\hat{\beta}_\perp^2, \omega_p^2/\omega_c^2)$  parameter space corresponding to stability and instability.

### B. Arbitrary energy anisotropy

Electromagnetic stability properties were examined in Sec. III A for the case of extreme energy anisotropy ( $\hat{\beta}_z=0$ ). In this section we make use of the electromagnetic dispersion relation (19) to investigate detailed stability properties for finite values of the anisotropy factor  $\hat{\beta}_\perp^2/2\hat{\beta}_z^2$ . In particular, Eq. (19) is solved numerically for the real oscillation frequency  $\text{Re}\omega$  and growth rate  $\text{Im}\omega$  for both the cyclotron maser and whistler branches over a

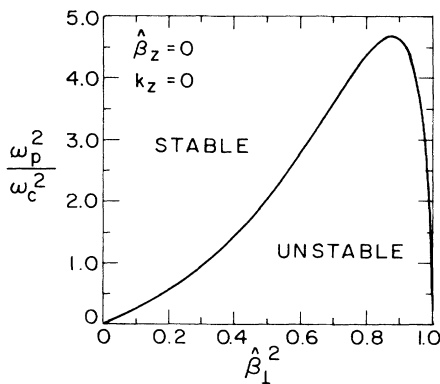


FIG. 4. Regions of  $(\hat{\beta}_\perp^2, \omega_p^2/\omega_c^2)$  parameter space corresponding to stability ( $\text{Im}\omega=0$ ) and instability ( $\text{Im}\omega>0$ ) for the cyclotron maser mode [Eqs. (27) and (28)]. For  $\hat{\beta}_z=0$  and specified  $\hat{\beta}_\perp^2 \neq 0$ , the cyclotron maser instability is absent for sufficiently large values of  $\omega_p^2/\omega_c^2$ .

wide range of system parameters  $\omega_p^2/\omega_c^2$  and  $\hat{\beta}_\perp^2/2\hat{\beta}_z^2$ .

Typical results are illustrated in Fig. 5 for the choice of system parameters  $\omega_p^2/\omega_c^2=0.25$  and  $\hat{\beta}_\perp^2=0.5$ . In Fig. 5(a) the normalized real oscillation frequency  $\text{Re}\omega/\omega_p$  is plotted versus  $ck_z/\omega_p$  for the case  $\hat{\beta}_\perp^2/2\hat{\beta}_z^2=11$ . The dashed portions of the dispersion curves in Fig. 5(a) correspond to the unstable range of wave numbers for the cyclotron maser and whistler instabilities. Further detail is presented in Figs. 5(b)–5(e). In particular, shown in Figs. 5(b) and 5(c) for the electron whistler branch are plots of  $\text{Re}\omega/\omega_p$  [Fig. 5(b)] and  $\text{Im}\omega/\omega_p$  [Fig. 5(c)] versus  $ck_z/\omega_p$  obtained from Eq. (19) for anisotropy factors ranging from  $\hat{\beta}_\perp^2/2\hat{\beta}_z^2=\infty$  to  $\hat{\beta}_\perp^2/2\hat{\beta}_z^2=1$ . We note from Fig. 5(c) that the maximum growth rate and the range of unstable  $k_z$  values decrease with decreasing values of  $\hat{\beta}_\perp^2/2\hat{\beta}_z^2$ . Moreover, there is a corresponding decrease in  $\text{Re}\omega/\omega_p$  as  $\hat{\beta}_\perp^2/2\hat{\beta}_z^2$  is reduced [Fig. 5(b)]. For  $\hat{\beta}_\perp^2=0.5$  and  $\omega_p^2/\omega_c^2=0.25$ , it is found from Eq. (19) that the whistler instability is completely stabilized when the anisotropy factor is reduced to  $\hat{\beta}_\perp^2/2\hat{\beta}_z^2=0.506$ . Finally, shown in Figs. 5(d) and 5(e) for the cyclotron maser branch are plots of  $\text{Re}\omega/\omega_p$  [Fig. 5(d)] and  $\text{Im}\omega/\omega_p$  [Fig. 5(e)] versus  $ck_z/\omega_p$  obtained from Eq. (19) for anisotropy factors ranging from  $\hat{\beta}_\perp^2/2\hat{\beta}_z^2=\infty$  to  $\hat{\beta}_\perp^2/2\hat{\beta}_z^2=0.51$ . We note from Fig. 5(d) that  $\text{Re}\omega/\omega_p$  decreases as the anisotropy factor  $\hat{\beta}_\perp^2/2\hat{\beta}_z^2$  is reduced. Moreover, the normalized growth rate  $\text{Im}\omega/\omega_p$  decreases as  $\hat{\beta}_\perp^2/2\hat{\beta}_z^2$  is reduced [Fig. 5(e)]. Indeed, for  $\hat{\beta}_\perp^2=0.5$  and  $\omega_p^2/\omega_c^2=0.25$ , it is found from Eq. (19) that complete stabilization of the cyclotron maser instability requires reduction of the anisotropy factor to  $\hat{\beta}_\perp^2/2\hat{\beta}_z^2=0.50$ , corresponding to  $\hat{\gamma} \rightarrow \infty$ . For general values of  $\hat{\beta}_\perp^2/2\hat{\beta}_z^2$ , we also note from Fig. 5(e) that maximum growth of the cyclotron maser instability occurs for  $k_z=0$  when  $k_\perp=0$ . (Compare with Fig. 2 for the special case where  $\hat{\beta}_z=0$ .)

Similar stability plots obtained from Eq. (19) are presented in Fig. 6 for the case where  $\hat{\beta}_\perp^2=0.5$  and the value of  $\omega_p^2/\omega_c^2$  is increased to  $\omega_p^2/\omega_c^2=5$ . For this choice of system parameters,  $\omega_p^2/\omega_c^2$  is sufficiently large that the cyclotron maser instability is absent ( $\text{Im}\omega=0$ ) for all values of the anisotropy factor  $\hat{\beta}_\perp^2/2\hat{\beta}_z^2$ . For the electron whistler branch,  $\text{Re}\omega/\omega_p$  and  $\text{Im}\omega/\omega_p$  are plotted versus  $ck_z/\omega_p$  in Figs. 6(a) and 6(b), respectively, for values of the anisotropy factor ranging from  $\hat{\beta}_\perp^2/2\hat{\beta}_z^2=\infty$  to  $\hat{\beta}_\perp^2/2\hat{\beta}_z^2=0.69$ . The qualitative features of the stability behavior in Fig. 6 are similar to Figs. 5(b) and 5(c), i.e., the real oscillation frequency, the growth rate, and the instability bandwidth (in  $k_z$  space) all decrease as the anisotropy factor  $\hat{\beta}_\perp^2/2\hat{\beta}_z^2$  is reduced. Moreover, we note that the normalized growth rates  $\text{Im}\omega/\omega_p$  in Fig. 6(b) (obtained for  $\omega_p^2/\omega_c^2=5$ ) are comparable in magnitude to those in Fig. 5(c) (obtained for  $\omega_p^2/\omega_c^2=0.25$ ). On the other hand, comparing Figs. 5(b) and 6(a), the real oscillation frequency (measured in units of  $\omega_p$ ) is reduced substantially as  $\omega_p^2/\omega_c^2$  is increased. For the choice of system parameters in Fig. 6, it is found from Eq. (19) that the whistler instability is completely stabilized when the anisotropy factor is reduced to  $\hat{\beta}_\perp^2/2\hat{\beta}_z^2=0.51$ .

For the cyclotron maser branch, Fig. 7 illustrates the scaling of stability properties with  $\omega_p^2/\omega_c^2$ . In particular,

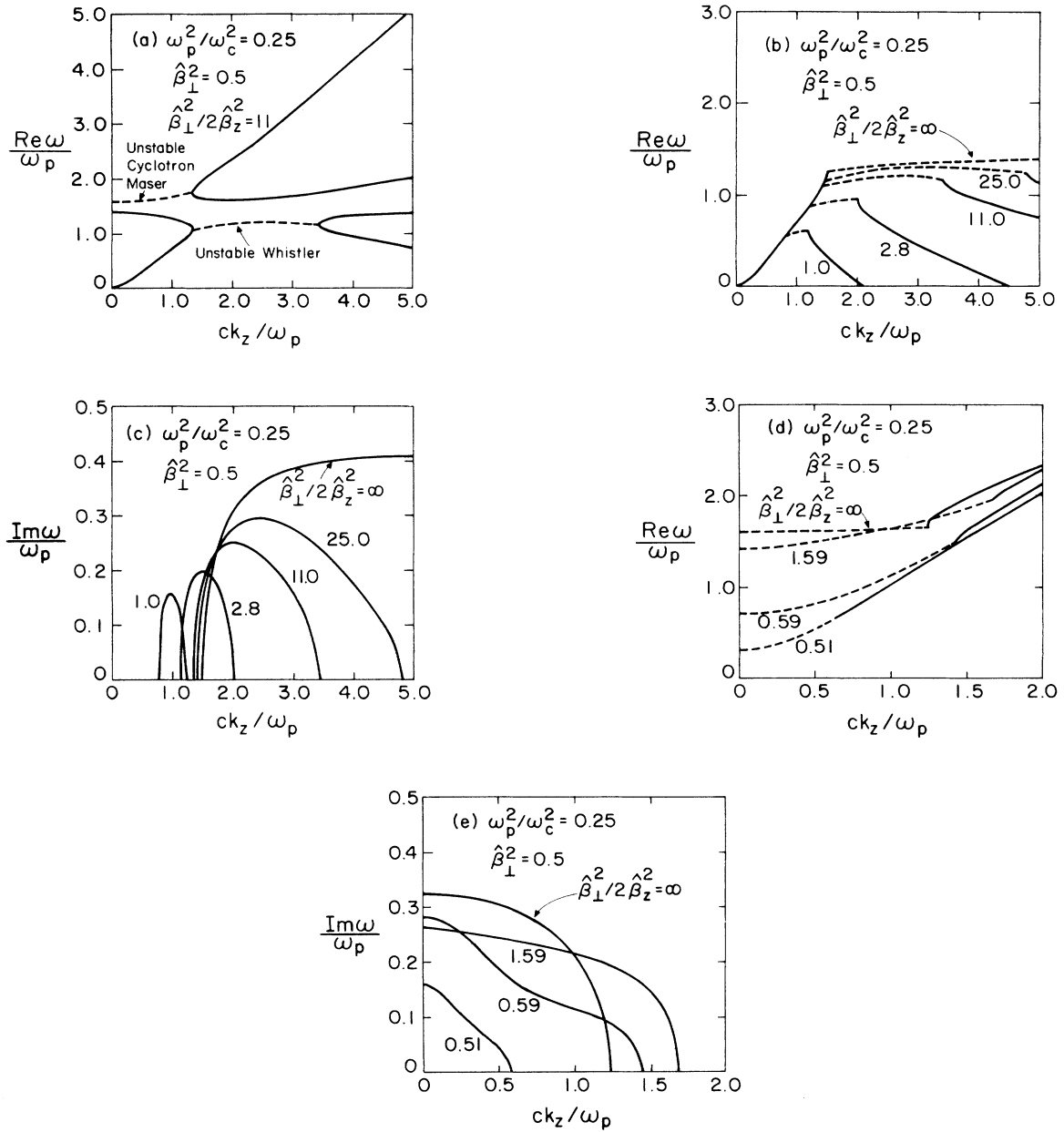


FIG. 5. Electromagnetic stability properties calculated from Eq. (19) for  $\hat{\beta}_1^2=0.5$  and  $\omega_p^2/\omega_c^2=0.25$ . Plots of (a)  $\text{Re}\omega/\omega_p$  vs  $ck_z/\omega_p$  for  $\hat{\beta}_1^2/2\hat{\beta}_z^2=11$ . Plots of (b)  $\text{Re}\omega/\omega_p$ , and (c)  $\text{Im}\omega/\omega_p$  vs  $ck_z/\omega_p$  for the whistler branch for several values of  $\hat{\beta}_1^2/2\hat{\beta}_z^2$ . Plots of (d)  $\text{Re}\omega/\omega_p$ , and (e)  $\text{Im}\omega/\omega_p$  vs  $ck_z/\omega_p$  for the cyclotron maser branch for several values of  $\hat{\beta}_1^2/2\hat{\beta}_z^2$ .

shown in Fig. 7 are plots of  $\text{Re}\omega/\omega_p$  [Fig. 7(a)] and  $\text{Im}\omega/\omega_p$  [Fig. 7(b)] versus  $ck_z/\omega_p$  obtained from Eq. (19) for  $\hat{\beta}_1^2=0.5$ ,  $\hat{\beta}_1^2/2\hat{\beta}_z^2=1.56$  (which corresponds to  $\hat{\beta}_z^2=0.160$  when  $\hat{\beta}_1^2=0.5$ ), and values of normalized density ranging from  $\omega_p^2/\omega_c^2=0.25$  to  $\omega_p^2/\omega_c^2=1$ . It is evident from Fig. 7 that the real oscillation frequency, growth rate, and bandwidth (in  $k_z$  space) all decrease as  $\omega_p^2/\omega_c^2$  is increased. Indeed, for the choice of system parameters in Fig. 7, the cyclotron maser instability is completely stabilized when the normalized density is increased to  $\omega_p^2/\omega_c^2=2.3$ .

Similarly, Fig. 8 shows the scaling of stability properties with  $\omega_p^2/\omega_c^2$  calculated from Eq. (19) for the whistler branch. In particular,  $\text{Re}\omega/\omega_p$  and  $\text{Im}\omega/\omega_p$  are plotted versus  $ck_z/\omega_p$  in Figs. 8(a) and 8(b), respectively, for the choice of system parameters  $\hat{\beta}_1^2=0.5$ ,  $\hat{\beta}_1^2/2\hat{\beta}_z^2=11$  (which corresponds to  $\hat{\beta}_z^2=0.0227$  when  $\hat{\beta}_1^2=0.5$ ), and values of normalized density ranging from  $\omega_p^2/\omega_c^2=0.25$  to  $\omega_p^2/\omega_c^2=25$ . We note that  $\text{Re}\omega/\omega_p$  decreases as  $\omega_p^2/\omega_c^2$  is increased [Fig. 8(a)], and there is a concomitant downshift in  $k_z$  of the growth rate curves [Fig. 8(b)]. Indeed, in the limit of zero magnetic field ( $\omega_p^2/\omega_c^2 \rightarrow \infty$ ), the

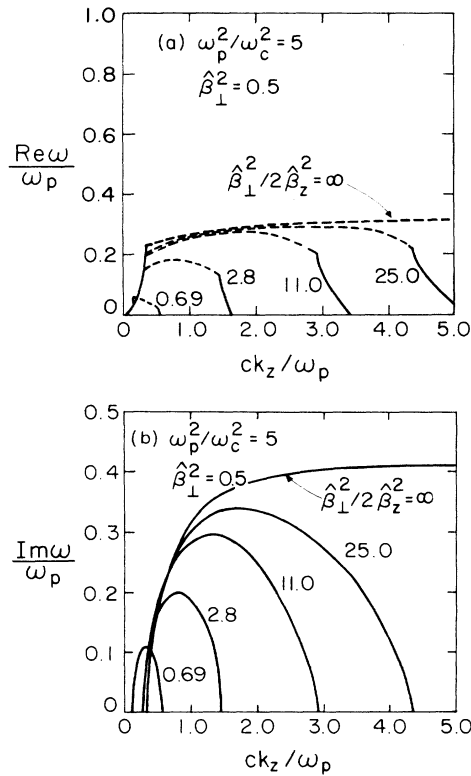


FIG. 6. Whistler stability properties calculated from Eq. (19) for  $\hat{\beta}_\perp^2=0.5$  and  $\omega_p^2/\omega_c^2=5$ . Plots of (a)  $\text{Re}\omega/\omega_p$ , and (b)  $\text{Im}\omega/\omega_p$  vs  $ck_z/\omega_p$  for several values of  $\hat{\beta}_\perp^2/2\hat{\beta}_z^2$ . (The cyclotron maser instability is absent for the choice of system parameters in Fig. 6.)

whistler instability in Fig. 8 evolves continuously into the classical Weibel instability<sup>20,22</sup> with  $\text{Re}\omega=0$ , and nonzero growth rate ( $\text{Im}\omega \neq 0$ ) over a finite bandwidth in  $k_z$  space.

The dispersion relation (19) can also be used to determine the stability boundaries separating the regions of parameter space corresponding to stability ( $\text{Im}\omega=0$ ) and instability ( $\text{Im}\omega>0$ ). Shown in Fig. 9 are the regions of  $(\hat{\beta}_\perp^2, \omega_p^2/\omega_c^2)$  parameter space corresponding to stability and instability for the cyclotron maser mode. The stability boundaries in Fig. 9 are calculated from Eq. (19) for several values of  $\hat{\beta}_z$ . For specified  $\hat{\beta}_z$ , the region above the curve in Fig. 9 corresponds to stability. As in the case  $\hat{\beta}_z=0$  (Fig. 4), for specified value of  $\hat{\beta}_\perp^2$ , it is evident from Fig. 9 that there exists a critical value of  $\omega_p^2/\omega_c^2$  above which the cyclotron maser instability is completely stabilized. Note also from Fig. 9 that the unstable region of  $(\hat{\beta}_\perp^2, \omega_p^2/\omega_c^2)$  parameter space continues to decrease in area as  $\hat{\beta}_z$  is increased and the anisotropy factor  $\hat{\beta}_\perp^2/2\hat{\beta}_z^2$  is reduced.

Finally, shown in Fig. 10 are the regions of  $(2\hat{\beta}_z^2, \hat{\beta}_\perp^2)$  parameter space corresponding to stability and instability for the whistler mode. The stability boundaries in Fig. 10 are calculated from Eq. (19) for several values of  $\omega_p^2/\omega_c^2$ . For specified  $\omega_p^2/\omega_c^2$ , the region above the curve starting at the origin in Fig. 10 corresponds to instability ( $\text{Im}\omega>0$ ). That is, the anisotropy factor  $\hat{\beta}_\perp^2/2\hat{\beta}_z^2$  is large

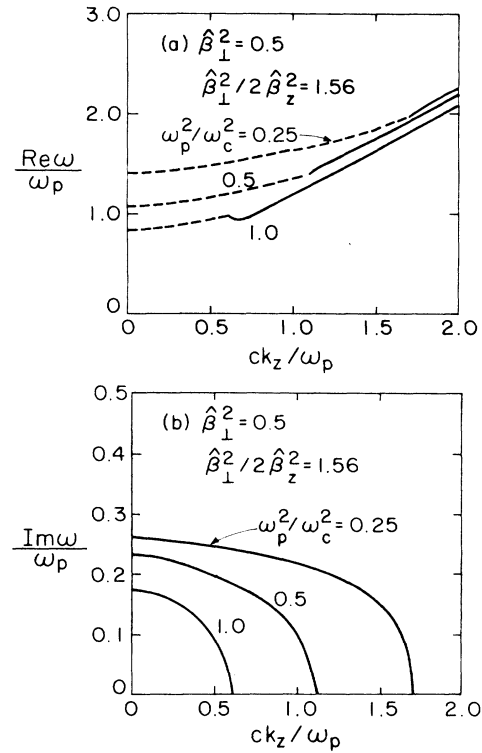


FIG. 7. Cyclotron maser stability properties calculated from Eq. (19) for  $\hat{\beta}_\perp^2=0.5$  and  $\hat{\beta}_\perp^2/2\hat{\beta}_z^2=1.56$ . Plots of (a)  $\text{Re}\omega/\omega_p$ , and (b)  $\text{Im}\omega/\omega_p$  vs  $ck_z/\omega_p$  for several values of  $\omega_p^2/\omega_c^2$ .

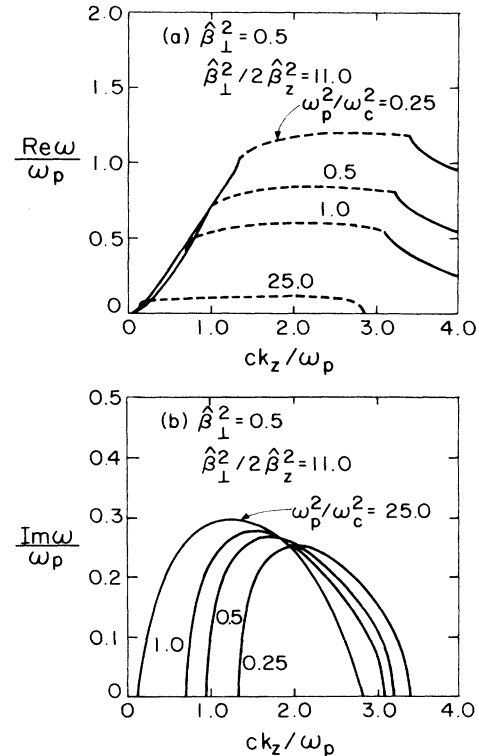


FIG. 8. Whistler stability properties calculated from Eq. (19) for  $\hat{\beta}_\perp^2=0.5$  and  $\hat{\beta}_\perp^2/2\hat{\beta}_z^2=11$ . Plots of (a)  $\text{Re}\omega/\omega_p$ , and (b)  $\text{Im}\omega/\omega_p$  vs  $ck_z/\omega_p$  for several values of  $\omega_p^2/\omega_c^2$ .



enough in this region to give instability. As  $\omega_p^2/\omega_c^2$  is decreased from  $\omega_p^2/\omega_c^2 = \infty$  (corresponding to  $B_0=0$ ), it is evident from Fig. 10 that smaller values of the anisotropy factor  $\hat{\beta}_1^2/2\hat{\beta}_z^2$  are required to stabilize the whistler instability.

#### IV. DISPERSION RELATION FOR THERMAL EQUILIBRIUM DISTRIBUTION IN PARALLEL MOMENTUM

For completeness, in this section we simplify the dispersion relation (4) for the case where the parallel-momentum

distribution  $F_1(p_z)$  corresponds to the thermal equilibrium distribution

$$F_1(p_z) = \frac{\exp(-\gamma mc^2/T_z)}{2\hat{\gamma}_1 mc K_1(\hat{\gamma}_1 mc^2/T_z)}. \quad (29)$$

Here,  $T_z = \text{const}$  is the parallel temperature,  $\gamma = (1 + \hat{p}_1^2/m^2 c^2 + p_z^2/m^2 c^2)^{1/2}$  is defined in Eq. (5),  $\hat{\gamma}_1 = (1 + \hat{p}_1^2/m^2 c^2)^{1/2}$  is defined in Eq. (12), and  $K_n(x)$  is the modified Bessel function of the second kind of order  $n$ . Substituting Eq. (29) into Eq. (4) gives the dispersion relation

$$0 = D_T^\pm(k_z, \omega) = 1 - \frac{c^2 k_z^2}{\omega^2} - \frac{(\omega_p^2/\omega^2)}{2\hat{\gamma}_1 mc K_1(\hat{\gamma}_1 mc^2/T_z)} \times \int_{-\infty}^{\infty} \frac{dp_z}{\gamma} \exp(-\gamma mc^2/T_z) \left[ \frac{\gamma\omega - k_z p_z/m}{\gamma\omega - k_z p_z/m \pm \omega_c} - \frac{\hat{p}_1^2}{2m^2 c^2} \frac{(\omega^2 - c^2 k_z^2)}{(\gamma\omega - k_z p_z/m \pm \omega_c)^2} \right], \quad (30)$$

where  $\text{Im}\omega > 0$  is assumed. We express Eq. (30) in an alternate form by making use of the identities (valid for  $\text{Im}\omega > 0$ )

$$\int_0^\infty d\tau \exp[i(\gamma\omega - k_z p_z/m \pm \omega_c)\tau] = \frac{i}{\gamma\omega - k_z p_z/m \pm \omega_c}, \quad (31)$$

$$\int_0^\infty d\tau \tau \exp[i(\gamma\omega - k_z p_z/m \pm \omega_c)\tau] = -\frac{1}{(\gamma\omega - k_z p_z/m \pm \omega_c)^2}.$$

We further introduce the transformation  $p_z = (\hat{\gamma}_1 mc) \sinh\alpha$  and  $\gamma = \hat{\gamma}_1 \cosh\alpha$  defined in Eqs. (14) and (15). Equation (30) can then be expressed in the equivalent form

$$0 = D_T^\pm(k_z, \omega) = 1 - \frac{c^2 k_z^2}{\omega^2} + \frac{i(\omega_p^2/\omega^2)}{2\hat{\gamma}_1 mc K_1(\hat{\gamma}_1 mc^2/T_z)} \times \int_0^\infty d\tau \exp[\pm i(\omega_c/\hat{\gamma}_1)\tau] \int_{-\infty}^\infty d\alpha \exp[-(\hat{\gamma}_1 mc^2/T_z - i\omega\tau)\cosh\alpha - ick_z\tau \sinh\alpha] \times \left[ \cosh\alpha - \frac{ck_z}{\omega} \sinh\alpha + i\omega\tau \left( 1 - \frac{c^2 k_z^2}{\omega^2} \right) \frac{\hat{p}_1^2}{2\hat{\gamma}_1^2 m^2 c^2} \right], \quad (32)$$

where use has been made of Eqs. (14), (15), and (31). The integration over  $\alpha$  in Eq. (32) can be carried out exactly by making use of the integral transform

$$\frac{1}{\pi} K_0((a^2 + b^2)^{1/2}) = \frac{1}{2\pi} \int_{-\infty}^\infty d\alpha \exp(-ib \sinh\alpha - a \cosh\alpha). \quad (33)$$

We introduce the variable  $\zeta$  defined by

$$\zeta^2 = \left[ \frac{\hat{\gamma}_1 mc^2}{T_z} - i\omega\tau \right]^2 + c^2 k_z^2 \tau^2. \quad (34)$$

Then, from Eqs. (33) and (34), the dispersion relation (32) can be expressed as

$$0 = D_T^\pm(k_z, \omega) = 1 - \frac{c^2 k_z^2}{\omega^2} - \frac{\omega_p^2/\hat{\gamma}_1}{\omega^2} \left[ \frac{K_0(\hat{\gamma}_1 mc^2/T_z)}{K_1(\hat{\gamma}_1 mc^2/T_z)} + \frac{i}{K_1(\hat{\gamma}_1 mc^2/T_z)} \int_0^\infty d\tau K_0(\zeta) \exp[\pm i(\omega_c/\hat{\gamma}_1)\tau] \times \left[ \pm \frac{\omega_c}{\hat{\gamma}_1} - i\tau(\omega^2 - c^2 k_z^2) \frac{\hat{p}_1^2}{2\hat{\gamma}_1^2 m^2 c^2} \right] \right] \quad (35)$$

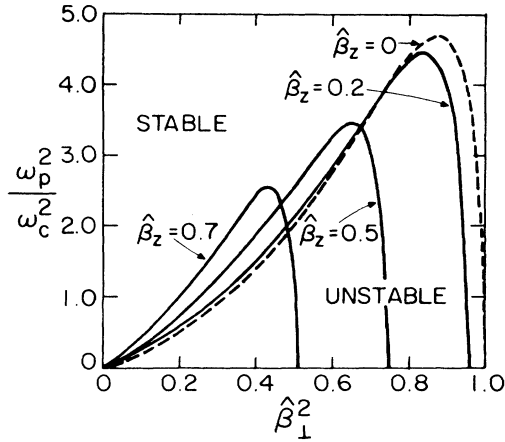


FIG. 9. Regions of  $(\hat{\beta}_\perp^2, \omega_p^2/\omega_c^2)$  parameter space corresponding to stability ( $\text{Im}\omega=0$ ) and instability ( $\text{Im}\omega>0$ ) for the cyclotron maser mode. The stability boundaries are calculated from Eq. (19) for several values of  $\hat{\beta}_z$  (see also Fig. 4).

for  $\text{Im}\omega>0$ . Although the  $\tau$  integration in Eq. (35) cannot be carried out in closed form, this form of the dispersion relation is particularly useful for numerical solutions and for analytical approximations in various limiting regimes. A detailed analysis of Eq. (35) will be the subject of a future investigation.

As a simple limiting case, we consider Eq. (35) for  $B_0=0$ , which corresponds to the Weibel instability in an unmagnetized plasma. Some straightforward algebra that makes use of Eqs. (3) and (29) shows that  $T_z$  can be identified with the parallel temperature  $\int d^3p(p_z^2/\gamma m)F(p_\perp^2, p_z)$ , and that the effective perpendicular temperature  $T_\perp = \int d^3p(p_\perp^2/2\gamma m)F(p_\perp^2, p_z)$  is given by

$$T_\perp = \frac{1}{2}\hat{\gamma}_\perp mc^2 \left[ \frac{\hat{p}_\perp}{\hat{\gamma}_\perp mc} \right]^2 \frac{K_0(\hat{\gamma}_\perp mc^2/T_z)}{K_1(\hat{\gamma}_\perp mc^2/T_z)}. \quad (36)$$

Setting  $\omega_c=0$  in Eq. (35) and making use of Eq. (36) gives the dispersion relation for an unmagnetized plasma, i.e.,

$$\begin{aligned} 0 &= D_T(k_z, \omega) \\ &= 1 - \frac{c^2 k_z^2}{\omega^2} \\ &\quad - \frac{(\omega_p^2/\hat{\gamma}_\perp)}{\omega^2} \left[ \frac{K_0(\hat{\gamma}_\perp mc^2/T_z)}{K_1(\hat{\gamma}_\perp mc^2/T_z)} \right. \\ &\quad \left. + \frac{T_\perp}{\hat{\gamma}_\perp mc^2} \frac{(\omega^2 - c^2 k_z^2)}{K_0(\hat{\gamma}_\perp mc^2/T_z)} \int_0^\infty d\tau \tau K_0(\xi) \right]. \end{aligned} \quad (37)$$

The  $\tau$  integral in Eq. (37) must generally be evaluated numerically, or in the context of asymptotic expansions for large or small values of  $|\xi|$ . Unlike Eq. (19), the disper-

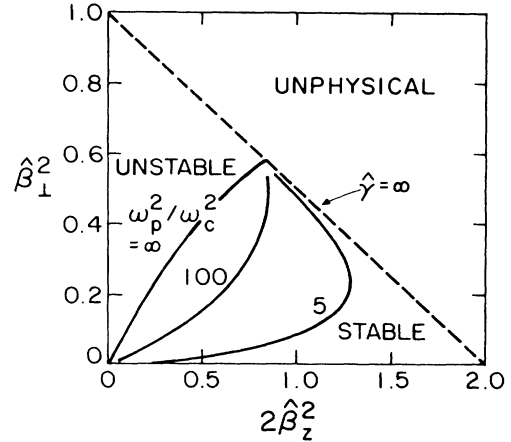


FIG. 10. Regions of  $(2\hat{\beta}_\perp^2, \hat{\beta}_\perp^2)$  parameter space corresponding to stability ( $\text{Im}\omega=0$ ) and instability ( $\text{Im}\omega>0$ ) for the whistler mode. The stability boundaries are calculated from Eq. (19) for several values of  $\omega_p^2/\omega_c^2$ .

sion relation (37) generally incorporates the effects of collisionless dissipation (Landau damping) by the  $p_z$  distribution in Eq. (29). For the slow-wave branch, it can be shown from Eq. (37) that the necessary and sufficient condition for instability is given by

$$\frac{T_\perp}{T_z} > \left[ \frac{K_0(\hat{\gamma}_\perp mc^2/T_z)}{K_1(\hat{\gamma}_\perp mc^2/T_z)} \right]^2, \quad (38)$$

where  $T_\perp$  is defined in Eq. (36). Moreover, when Eq. (38) is satisfied, it is found that  $\text{Re}\omega=0$  (for the slow-wave branch) over the range of unstable wave numbers specified by

$$0 < k_z^2 < k_0^2 \equiv \frac{\omega_p^2}{\hat{\gamma}_\perp c^2} \left[ \frac{T_\perp}{T_z} \frac{K_1(\hat{\gamma}_\perp mc^2/T_z)}{K_0(\hat{\gamma}_\perp mc^2/T_z)} - \frac{K_0(\hat{\gamma}_\perp mc^2/T_z)}{K_1(\hat{\gamma}_\perp mc^2/T_z)} \right]. \quad (39)$$

Note from Eq. (39) that the marginal stability point  $k_0^2$  (where  $\text{Im}\omega=0=\text{Re}\omega$ ) can be calculated in closed analytical form. This follows from the identity

$$\lim_{\text{Im}\omega \rightarrow 0^+} \left[ c^2 k_z^2 \int_0^\infty d\tau \tau K_0(\xi) \right]_{\text{Re}\omega=0} = \frac{\hat{\gamma}_\perp mc^2}{T_z} K_1(\hat{\gamma}_\perp mc^2/T_z). \quad (40)$$

Finally, shown in Fig. 11 is a plot of the stability boundary in the parameter space  $(T_z/\hat{\gamma}_\perp mc^2, T_\perp/\hat{\gamma}_\perp mc^2)$  calculated numerically from Eq. (38). The region above the curve in Fig. 11 corresponds to instability, which requires sufficiently large thermal anisotropy  $T_\perp/T_z$ .

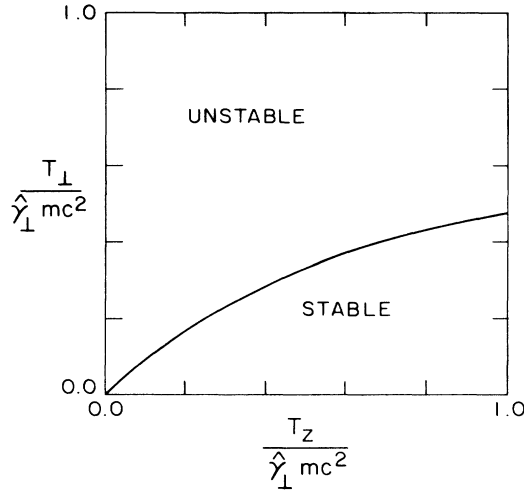


FIG. 11. Regions of  $(T_z/\hat{\gamma}_1 mc^2, T_\perp/\hat{\gamma} mc^2)$  parameter space corresponding to stability ( $\text{Im}\omega=0$ ) and instability ( $\text{Im}\omega>0$ ) for the slow-wave (Weibel) mode. The stability boundary is calculated from Eqs. (37) and (38) ( $B_0=0$ ).

## V. CONCLUSIONS

For the case of parallel propagation, detailed properties of the cyclotron maser and whistler instabilities in a relativistic magnetized plasma have been investigated for the particular choice of  $F(p_\perp^2, p_z)$  in Eq. (7), which permits an exact analytical reduction of the dispersion relation (2) for arbitrary energy anisotropy (Sec. II). The resulting dispersion relation in Eq. (19) was solved numerically, and detailed properties of the cyclotron maser and whistler instabilities were determined over a wide range of effective energy anisotropy  $\hat{\beta}_\perp^2/2\hat{\beta}_z^2$  and normalized density  $\omega_p^2/\omega_c^2$  (Sec. III). Not only does the choice of waterbag distribu-

tion in Eq. (7) readily permit the calculation of detailed stability properties over a wide range of system parameters, the corresponding dispersion relation (19) can be used to determine universal stability boundaries for the cyclotron maser and whistler instabilities. For example, Figs. 4 and 9 show the stability boundaries for the cyclotron maser instability in  $(\hat{\beta}_\perp^2, \omega_p^2/\omega_c^2)$  parameter space for several values of  $\hat{\beta}_z$ . Similarly, the stability boundaries for the whistler instability in  $(2\hat{\beta}_z^2, \hat{\beta}_\perp^2)$  parameter space are illustrated in Fig. 10 for several values of  $\omega_p^2/\omega_c^2$ . Finally, the electromagnetic dispersion relation (35) was derived for the case where the parallel momentum distribution  $F_1(p_z)$  corresponds to the thermal equilibrium distribution in Eq. (29) (Sec. IV).

## ACKNOWLEDGMENTS

This research was supported in part by the U.S. Department of Energy and in part by the U.S. Office of Naval Research.

## APPENDIX: EVALUATION OF AXIAL MOMENTUM INTEGRALS

We evaluate here the integrals over  $\alpha$  required to simplify the dispersion relation (16). In this regard, it is useful to introduce the definite integrals defined by

$$I_1 \equiv \int_{-\hat{\alpha}}^{\hat{\alpha}} \frac{d\alpha}{(a+b \cosh\alpha + d \sinh\alpha)}, \quad (\text{A1})$$

$$I_2 \equiv \int_{-\hat{\alpha}}^{\hat{\alpha}} d\alpha \frac{(b \cosh\alpha + d \sinh\alpha)}{(a+b \cosh\alpha + d \sinh\alpha)}, \quad (\text{A2})$$

$$I_3 \equiv \int_{-\hat{\alpha}}^{\hat{\alpha}} \frac{d\alpha}{(a+b \cosh\alpha + d \sinh\alpha)^2}, \quad (\text{A3})$$

where  $\sinh\hat{\alpha} = \hat{p}_z/\hat{\gamma}_1 mc$ ,  $a = \pm\omega_c/\hat{\gamma}_1\omega$ ,  $b=1$ , and  $d = -ck_z/\omega$ . Some straightforward algebra shows that

$$\begin{aligned} I_1 &= \frac{1}{(a^2+d^2-b^2)^{1/2}} \ln \left[ \frac{(a-b)\tanh(\alpha/2) - d + (a^2+d^2-b^2)^{1/2}}{(a-b)\tanh(\alpha/2) - d - (a^2+d^2-b^2)^{1/2}} \right] \Bigg|_{-\hat{\alpha}}^{\hat{\alpha}} \\ &= \frac{\omega(1-\hat{\beta}_z^2)^{1/2}}{[(\omega_c/\hat{\gamma})^2 + (1-\hat{\beta}_z^2)(c^2k_z^2 - \omega^2)]^{1/2}} \ln \left[ \frac{\omega(1-\hat{\beta}_z^2) \pm \omega_c/\hat{\gamma} + \hat{\beta}_z[(\omega_c/\hat{\gamma})^2 + (1-\hat{\beta}_z^2)(c^2k_z^2 - \omega^2)]^{1/2}}{\omega(1-\hat{\beta}_z^2) \pm \omega_c/\hat{\gamma} - \hat{\beta}_z[(\omega_c/\hat{\gamma})^2 + (1-\hat{\beta}_z^2)(c^2k_z^2 - \omega^2)]^{1/2}} \right]. \end{aligned} \quad (\text{A4})$$

Moreover, from Eqs. (A1) and (A2),  $I_2$  can be expressed in terms of  $I_1$  by

$$I_2 = 2\hat{\alpha} - aI_1. \quad (\text{A5})$$

Making use of  $\sinh\hat{\alpha} = \hat{p}_z/\hat{\gamma}_1 mc = (\hat{\gamma}/\hat{\gamma}_1)\hat{\beta}_z = (\cosh\hat{\alpha})\hat{\beta}_z$  gives  $2\hat{\alpha} = \ln[(1+\hat{\beta}_z)/(1-\hat{\beta}_z)]$ . For  $a = \pm\omega_c/\hat{\gamma}_1\omega$ , Eq. (A5) then becomes

$$I_2 = \ln \left[ \frac{1+\hat{\beta}_z}{1-\hat{\beta}_z} \right] \mp \frac{\omega_c/\hat{\gamma}}{\omega(1-\hat{\beta}_z^2)^{1/2}} I_1, \quad (\text{A6})$$

where  $I_1$  is defined in Eq. (A4). Finally, making use of Eq. (A3), it can be shown that  $I_3$  can be expressed as

$$\begin{aligned} I_3 &= -\frac{(1-\hat{\beta}_z^2)}{2\hat{\beta}_z} \frac{\omega^2}{[\omega_c^2/\hat{\gamma}^2 + (1-\hat{\beta}_z^2)(c^2k_z^2 - \omega^2)]} \\ &\quad \times \left[ \frac{\omega(\omega \pm \omega_c/\hat{\gamma}) - c^2k_z^2}{(\omega \pm \omega_c/\hat{\gamma})^2 - c^2k_z^2 \hat{\beta}_z^2} \right] \\ &\quad \pm \frac{\omega(\omega_c/\hat{\gamma})(1-\hat{\beta}_z^2)^{1/2}}{\omega_c^2/\hat{\gamma}^2 + (1-\hat{\beta}_z^2)(c^2k_z^2 - \omega^2)} I_1, \end{aligned} \quad (\text{A7})$$

where  $I_1$  is defined in Eq. (A4), and  $\hat{\gamma}$  is defined by

$$\hat{\gamma} = (1 + \hat{p}_1^2/m^2c^2 + \hat{p}_z^2/m^2c^2)^{1/2}.$$

Substituting the expressions for  $I_1$ ,  $I_2$ , and  $I_3$  in Eqs. (A4), (A6), and (A7) into Eq. (16) gives the desired disper-

sion relation in Eq. (19). From the expression for  $G(\xi)$  in Eq. (21), we note that the following expansions for  $G(\xi)$  pertain:

$$G(\xi) = \begin{cases} 1 + \frac{\xi^2}{3} + \frac{\xi^4}{5} + \cdots + \frac{\xi^{2n}}{(2n+1)} + \cdots, & |\xi| < 1, \\ \frac{1}{\xi^2} + \frac{1}{3\xi^4} + \frac{1}{5\xi^6} + \cdots + \frac{1}{(2n+1)\xi^{2n+2}} + \cdots + i\frac{\pi}{2\xi}, & |\xi| > 1, \end{cases} \quad (\text{A8})$$

in the regions  $|\xi| < 1$  and  $|\xi| > 1$ .

- <sup>1</sup>K. R. Chu and J. L. Hirschfield, *Phys. Fluids* **21**, 461 (1978).  
<sup>2</sup>H. S. Uhm, R. C. Davidson, and K. R. Chu, *Phys. Fluids* **21**, 1866 (1978).  
<sup>3</sup>C. S. Wu and L. C. Lee, *Astrophys. J.* **230**, 621 (1979).  
<sup>4</sup>L. C. Lee and C. S. Wu, *Phys. Fluids* **23**, 1348 (1980).  
<sup>5</sup>S. T. Tsai, C. S. Wu, Y. D. Wang, and S. W. Kang, *Phys. Fluids* **24**, 2186 (1981).  
<sup>6</sup>C. S. Wu, C. S. Lin, H. K. Wong, S. T. Tsai, and R. L. Zhou, *Phys. Fluids* **24**, 2191 (1981).  
<sup>7</sup>R. M. Winglee, *Plasma Phys.* **25**, 217 (1982).  
<sup>8</sup>H. K. Wong, C. S. Wu, F. J. Ke, R. S. Schneider, and L. F. Ziebell, *J. Plasma Phys.* **28**, 503 (1982).  
<sup>9</sup>Y. Y. Lau and K. R. Chu, *Phys. Rev. Lett.* **50**, 243 (1983).  
<sup>10</sup>D. Le Quéau, R. Pellat, and A. Roux, *Phys. Fluids* **27**, 247 (1984).  
<sup>11</sup>P. L. Pritchett, *Phys. Fluids* **27**, 2393 (1984).  
<sup>12</sup>H. K. Wong, C. S. Wu, and J. D. Gaffey, Jr., *Phys. Fluids* **28**,

- 2751 (1985).  
<sup>13</sup>R. M. Winglee, *Astrophys. J.* **291**, 160 (1985).  
<sup>14</sup>P. L. Pritchett, *Phys. Fluids* **29**, 2919 (1986).  
<sup>15</sup>H. S. Uhm and R. C. Davidson, *Phys. Fluids* **29**, 2713 (1986).  
<sup>16</sup>K. T. Tsang, *Phys. Fluids* **27**, 1659 (1984).  
<sup>17</sup>R. N. Sudan, *Phys. Fluids* **6**, 57 (1963).  
<sup>18</sup>C. F. Kennel and H. E. Petscheck, *J. Geophys. Res.* **72**, 3303 (1967).  
<sup>19</sup>N. T. Gladd, *Phys. Fluids* **26**, 974 (1983), and references therein.  
<sup>20</sup>R. C. Davidson, *Handbook of Plasma Physics*, edited by A. A. Galeev and R. N. Sudan (North-Holland, New York, 1983), Vol. 1, pp. 521–585, cf., pp. 552–573, and references therein.  
<sup>21</sup>E. S. Weibel, *Phys. Rev. Lett.* **2**, 83 (1959).  
<sup>22</sup>P. H. Yoon and R. C. Davidson, *Phys. Rev. A* **35**, 2718 (1987).